β-arrestin1 mediates metastatic growth of breast cancer cells by facilitating HIF-1-dependent VEGF expression

Sudha K. Shenoy[1,2,§], **Sang-oh Han**[1], **Yu Lin Zhao**[3], **Makoto R. Hara**[1], **Timothy Oliver**[2], **Yiting Cao**[3], and **Mark W. Dewhirst**[3]

[1] Department of Medicine, Duke University Medical Center, Box 103204, Durham, North Carolina 27710 Phone: (919) 681-5061; Fax (919) 681-7851

[2] Department of Cell Biology, Duke University Medical Center, Box 103204, Durham, North Carolina 27710 Phone: (919) 681-5061; Fax (919) 681-7851

[3] Department of Radiation Oncology, Duke University Medical Center, Box 103204, Durham, North Carolina 27710 Phone: (919) 681-5061; Fax (919) 681-7851

Abstract

β-arrestins 1 and 2 are multifunctional adaptor proteins originally discovered for their role in desensitizing seven-transmembrane receptor signaling via the heterotrimeric guanine nucleotide binding proteins. Recently identified roles of β-arrestins include regulation of cancer cell chemotaxis and proliferation. Herein we report that β-arrestin1 expression regulates breast tumor colonization in nude mice and cancer cell viability during hypoxia. β-arrestin1 robustly interacts with nuclear hypoxia-induced factor 1α (HIF-1α) that is stabilized during hypoxia and potentiates HIF-1-dependent transcription of the angiogenic factor VEGF-A. Increased expression of β-arrestin1 in human breast cancer (infiltrating ductal carcinoma or IDC and metastatic IDC) correlates with increased levels of VEGF-A. While the anti-angiogenic drug thalidomide inhibits HIF-1-dependent *VEGF* transcription in breast carcinoma cells, it does not prevent HIF-1α stabilization, but leads to aberrant localization of HIF-1α to the perinuclear compartments and surprisingly stimulates nuclear export of β-arrestin1. Additionally, imatinib mesylate that inhibits release of VEGF induces nuclear export of β-arrestin1-HIF-1α complexes. Our findings suggest that β-arrestin1 regulates nuclear signaling during hypoxia to promote survival of breast cancer cells via VEGF signaling and that drugs that induce its translocation from the nucleus to the cytoplasm could be useful in anti-angiogenic and breast cancer therapies.

Keywords

Arrestin; HIF-1; VEGF; hypoxia

§Corresponding author, Sudha K. Shenoy: sudha@receptor-biol.duke.edu.

Conflict of interest

The authors declare no conflict of interest.

INTRODUCTION

β-arrestin1 (aka arrestin2) and β-arrestin2 (aka arrestin3) are ubiquitously expressed multifunctional signaling adaptor proteins originally discovered for their role in desensitizing seven-transmembrane G protein-coupled receptors (GPCRs or 7TMRs) (Lefkowitz & Shenoy, 2005). β-arrestins regulate both GPCR and non-GPCR pathways, under normal as well as pathological conditions including cancer (Lefkowitz et al., 2006). The two β-arrestin isoforms share roughly 70% sequence identity and in general perform similar functions in GPCR regulation (for example, receptor desensitization) (Lefkowitz & Shenoy, 2005). Studies utilizing siRNA-mediated depletion and individual isoform repletion of β-arrestin1/2 null mouse embryonic fibroblasts have revealed differential roles in the extent of their endocytic and signaling functions with respect to some GPCRs and the two isoforms can sometimes function in a reciprocal manner to regulate GPCR signaling (DeWire et al., 2007). Of the two β-arrestin isoforms, β-arrestin2 is excluded from the nucleus due to the presence of a Nuclear Export Signal (NES), that is absent in β-arrestin1 (Kang et al., 2005; Scott et al., 2002; Wang et al., 2003).

Previous studies indicate that both β-arrestins play a crucial role in mitogenic signaling and chemotaxis of cancer cells (Alvarez et al., 2009; Buchanan et al., 2006; Dasgupta et al., 2006; Ge et al., 2004; Girnita et al., 2007; Li et al., 2009; Raghuwanshi et al., 2008; Rosano et al., 2009; Zou et al., 2008). In a human colorectal carcinoma cell line, β-arrestin1 mediated c-Src activation was found to be necessary for the transactivation of the growth factor receptor EGFR and downstream AKT activation as well as for cellular chemotaxis *in vitro* (Buchanan et al., 2006). Transgenic overexpression of β-arrestin1 leads to rapid tumor progression and increased angiogenesis in mice (Zou et al., 2008). β-arrestin2 facilitates the rapid endocytosis of vascular endothelial cadherin in response to vascular endothelial growth factor (VEGF) stimulation leading to endothelial cell permeability (Gavard & Gutkind, 2006). β-arrestin2 also mediates endocytosis and downregulation of transforming growth factor-beta type III receptor and low levels of this receptor are correlated with cancer invasiveness (Mythreye & Blobe, 2009). Recent studies have shown that β-arrestin2 specifically acts as a repressor of androgen receptor activity in prostate cancer cells (Lakshmikanthan et al., 2009) and β-arrestin2 KO mice display enhanced lung tumor metastasis (Raghuwanshi et al., 2008). Thus, there is increasing evidence that β-arrestin1 is associated with cell invasion and proliferation in multiple types of tumors, while β-arrestin2 is bifunctional and promotes or represses specific cancers. While the overexpression of β-arrestin1 accelerates tumor progression in mice, it is unclear whether endogenous β-arrestin1 expression and/or activity are correlated with malignancy.

Malignant transformation of breast tumors involves up-regulation of angiogenic factors resulting from tumor hypoxia. Additionally, localized hypoxia in tumors renders them resistant to radiation and chemotherapy. The hypoxia-inducible factor-1 (HIF-1) is recognized as the master transcriptional switch during hypoxia, and activates >100 genes crucial for the cellular adaptation to low oxygen tension (Semenza, 2007). The HIF-1 transcription factor is a heterodimer consisting of the oxygen-regulated HIF-1α subunit and oxygen-insensitive HIF-1β subunit (aka aryl hydrocarbon receptor nuclear translocator, ARNT) (Wang et al., 1995). Under normoxia, HIF-1α is hydroxylated at specific proline

residues, which leads to its ubiquitination by the E3 ubiquitin ligase and tumor suppressor pVHL (Maxwell et al., 1999). Consequently, HIF-1α subunit is continuously degraded by the 26S proteasome. During hypoxia, prolyl hydroxylation does not occur and hence HIF-1α is not ubiquitinated and degraded. Stabilized HIF-1α translocates into the nucleus, heterodimerizes with HIF-1β to form a functional transcription factor and binds to specific promoter regions known as hypoxia responsive elements (HRE) to induce transcription of many genes especially those required for angiogenesis (e.g. VEGF), cell survival (e.g. insulin-like growth factor, IGF2), glucose metabolism (e.g. glucose transporter, GLUT1) and invasion (e.g. transforming growth factor α, TGFα) (Semenza, 2007). It is also suggested that optimal HIF-1 activity requires p300 binding (Arany et al., 1996) and might involve other juxtaposed transcriptional elements such as AP-1 (Kvietikova et al., 1995).

Herein, we report a novel interaction between β-arrestin1 and HIF-1α occurring in breast carcinoma cells and further show that this interaction is crucial for HIF-1 dependent gene transcription. We find a positive correlation between β-arrestin1 and VEGF-A expression levels in metastatic human breast cancer tissues, suggesting that β-arrestin1-dependent signaling during adaptation to hypoxia regulates breast tumor metastasis.

RESULTS

β-arrestin1 is up-regulated in invasive breast carcinoma

In the human genome, the β-arrestin1 gene maps to chromosome locus 11q13, which is often amplified in breast cancer (Chuaqui et al., 1997; Letessier et al., 2006). While β-arrestin1 overexpression promotes tumor growth in mice (Zou et al., 2008), transcriptome and gene profiling studies do not identify an increase in β-arrestin mRNA in breast cancer (Ma et al., 2003; Minn et al., 2005; Niida et al., 2009). On the other hand, we have found a dramatic increase in β-arrestin1 protein levels in invasive breast carcinoma cells (MDAMB-231) when compared with non invasive cells (HEK-293) and normal breast epithelial cells (Hs 578Bst, ATCC) (Fig 1A–C). β-arrestin2 is also expressed in MDAMB-231, but at much lower levels than in both HEK-293 and Hs 578Bst. Additionally in the above noninvasive cells, β-arrestin2 is the more abundant isoform.

We next analyzed the β-arrestin1 protein levels in normal and cancer tissue cores (MaxArray™ human breast carcinoma tissue microarray slides) by immunostaining with anti-βarrestin1 antibody (A1CT). About 70% of the IDC tissue sections analyzed had increased levels of β-arrestin1 and its expression was significantly higher in IDC than in normal breast specimens (Fig 1D–E). Qualitatively similar immunostaining patterns were obtained with a second β-arrestin1 specific antibody (BD Biosciences), but very weak signals were observed with secondary antibody alone or with the anti-β-arrestin2 A2CT (Fig S1). Hence, the β-arrestin isoform detected in these tissues is predominantly β-arrestin1.

β-arrestin knockdown retards colonization and growth of breast carcinoma cells in experimental metastasis assays

Previous studies have indicated that both β-arrestins 1 and 2 are required for chemotaxis of breast cancer cells (Ge et al., 2004), thereby suggesting that both isoforms might regulate

spread of cancer *in vivo*. Accordingly, we transfected MDAMB-231 cells stably expressing luciferase (231-luc) with either control siRNA or β-arrestin1/2 specific siRNA, injected the cells via tail vein into female nude mice, and performed bioluminescence imaging (Xenogen™ *in vivo* imaging systems) to track metastatic spread of cancer. After tail vein injections, we detected and quantified the signals *in vivo* over a period of 5 weeks using the Living Image acquisition and analysis software (Living Image®, Xenogen). Although the uptake of both control and β-arrestin1/2 knockdown cells in the lungs was similar at 24 hours, stable lung colonization was observed only in control-treated mice but not in mice that received β-arrestin-depleted cells (Fig 2A–B). Aliquots of cells used for the injection were immunoblotted for β-arrestin1/2 levels and analyzed for luciferase expression. As depicted in Fig 2C–D, β-arrestin1/2 knockdown cells had 15–20% more luciferase activity than control cells and β-arrestins 1 and 2 were completely knocked down. Additionally, we tested the effect of β-arrestin1 knockdown on the metastatic spread of murine breast cancer cells (4T1) that cause more aggressive tumor metastasis than MDAMB-231 cells in nude mice models. Tail-vein injection of 4T1 cells depleted of β-arrestin1 expression (~80% knockdown) led to delayed tumor growth and an increase in the survival of nude mice (Fig 2E–F). These data corroborate previous reports that β-arrestins 1 and 2 are critical for tumor metastasis, and identify that β-arrestins1 and/or 2 are required for viability of breast cancer cells *in vivo*. Additionally, the experiments with 4T1 cells convey a critical role for β-arrestin1 in breast cancer progression.

β-arrestin1 expression is critical for the viability of breast carcinoma cells under hypoxic stress

To discern whether expression of β-arrestins 1 and 2 affects cancer cell viability, we performed CellTiter-Glo® (Promega) luminescent cell viability assay on breast carcinoma cells transfected with siRNA targeting no mRNA (control), β-arrestin1 or β-arrestin2. This assay is based on the quantification of the cellular ATP present, which indicates the presence of metabolically active cells. Under normoxia, no significant differences were observed between control and β-arrestin knockdown cells suggesting that the general cell viability is unaffected by the depletion of β-arrestin1 or 2. Interestingly, when we treated the cells for 24 hours with 100 μM Cobalt Chloride ($CoCl_2$) a well-accepted hypoxia mimetic (Wang & Semenza, 1995), or induced hypoxia by growing cells in low (1%) oxygen, cell viability was significantly reduced in β-arrestin1- but not β-arrestin2- depleted cells when compared with cells transfected with control siRNA (Fig 3). It is known that cancer cells undergo genetic and adaptive changes that allow their survival in a hypoxic environment. Above findings suggest that β-arrestin1 expression facilitates cell survival during hypoxia by influencing adaptive gene programming via its signaling roles.

β-arrestin1 interacts with the oxygen-regulated transcription factor HIF-1α

Based on the effect of β-arrestin1 knockdown on cell survival during hypoxia (Fig 3), and on the knowledge about its nuclear localization and nuclear function in forming a complex with p300 that regulates HIF-1 activity (Arany et al., 1996, Kang et al., 2005), we hypothesized that β-arrestin1 could be modulating the transcriptional activity of HIF-1α, thus regulating the survival of breast carcinoma cells during hypoxia.

To assess whether the β-arrestin-HIF-1α interaction occurs in cells expressing endogenous amounts of the two proteins, we prepared extracts from MDAMB-231 cells that were treated with vehicle or $CoCl_2$ and tested the interaction by immunoprecipitation and immunoblotting. β-arrestin1 was detected in HIF-1α IPs but not in IPs with control IgG (Fig 4A). β-arrestin-HIF-1α binding was also detected in β-arrestin IPs isolated from nuclear extracts of MDAMB-231 cells after $CoCl_2$ treatment (Fig 4B). Furthermore, we detected colocalization of β-arrestin1 and HIF-1α in the nuclei of $CoCl_2$-treated MDAMB-231 cells upon immunostaining and confocal microscopy (Fig 4C). The exclusive cytoplasmic distribution of β-arrestin2 is attributed to the presence of a nuclear export signal (NES) that is absent in β-arrestin1 (Scott et al., 2002; Wang et al., 2003). Introduction of this NES in β-arrestin1 (βarr1Q394L) changes its subcellular distribution to be totally cytoplasmic (Wang et al., 2003). When we compared β-arrestin1, β-arrestin1Q394L and β-arrestin2 for their binding to HIF-1α, only the wild type β-arrestin1 formed a robust complex with HIF-1α (Fig 4D–E). These findings establish that both β-arrestin1 and HIF-1α interact in the nuclear compartment of breast cancer cells during hypoxia.

β-arrestin1 regulates the transcriptional activity of HIF-1α

To test if the above β-arrestin1-HIF-1α interaction has functional consequences, we analyzed the effect of β-arrestin1 expression on HIF-1-mediated transcription during hypoxia. One of the most characterized HIF-dependent genes is the potent endothelial mitogen, VEGF-A, which regulates endothelial cell proliferation and blood vessel formation in both normal and cancerous tissues (Liu et al., 1995). The *VEGF-A* gene contains a HRE in its 5′ UTR (untranslated region) and hypoxia induces a rapid and sustained increase in VEGF-A mRNA levels. To assess if HIF-1-dependent VEGF induction involves β-arrestin, we used a luciferase reporter system in which hypoxia-responsive elements (5XHRE) derived from the 5′ UTR of the human VEGF gene is ligated upstream of the firefly luciferase gene (Fig 5A). 5XHRE reporter transfection alone led to some basal promoter activity in MDAMB-231 cells. Nonetheless, treatment of cells with $CoCl_2$ or reduced oxygen levels (1%) significantly increased the luciferase activity (Fig 5B). This hypoxia-induced increase was not observed in cells with β-arrestin1 or β-arrestin1/2 knockdown whereas β-arrestin2 depletion did not significantly change reporter activity (Fig 5B–C). These data suggest that HIF-1 dependent transcriptional activity during hypoxia is regulated specifically by β-arrestin1 expression in MDAMB-231 cells. Additionally, we tested HIF-1α mediated transcriptional activity under β-arrestin1 null and replete conditions in a β-arrestin1/2 double knockout cell line (Kohout et al., 2001). Although we found a 1.8 fold $CoCl_2$-induced increase in HIF-1 transcriptional response in these β-arrestin null fibroblasts, restoration of β-arrestin1 expression led to a dramatic increase (6–7 fold) in HIF- mediated transcription during hypoxia (Fig 5D–E). Thus, β-arrestin1 augments HIF-1 directed transcription and there could be potential β-arrestin1-dependent signals with vital roles during hypoxia.

Increase in VEGF levels in invasive ductal carcinoma correlates with increase in β-arrestin1 levels

Because we observed an increase in β-arrestin1 expression in IDCs (Fig 1), and because β-arrestin1 expression correlated with HIF-1 transcriptional activity in MDAMB-231 cells

(Fig 5), we wondered if this would be reflected in the levels of either HIF-1α or the downstream target of HIF-1, VEGF-A, in IDCs. We analyzed β-arrestin1 and VEGF protein expression by immunostaining with the antibodies anti-β-arrestin1 (A1CT) and anti-VEGF-A (mouse monoclonal C-1), followed by respective secondary antibodies, one conjugated to Alexa Fluor® 488 and the other to Alexa Fluor® 594 (see methods). A representative set of confocal images for normal, IDC and metastatic IDC is shown in Fig 6A. The data acquired for β-arrestin1 and VEGF immunostaining for normal breast (n=10 tissue samples, 22 images), IDC (n=79 tissue samples, 112 images) and metastatic carcinoma in lymph node (n= 7 tissue samples, 12 images) is summarized as bar graphs in Fig 6B. Although VEGF expression varied from undetectable to very high levels among the different cancer samples, overall both β-arrestin1 and VEGF levels were significantly higher ($p < 0.01$) in IDC samples than in normal breast tissues. Despite various immunostaining attempts with available HIF-1α antibodies, we were unable to detect a specific signal for this protein in these breast tissue arrays. Additionally, although there was no direct relationship between the increase in β-arrestin1 and presence of estrogen receptor, progesterone receptor or expression of p53 in these IDC samples (Supplementary Table 1), we found a positive correlation between β-arrestin1 expression and VEGF-A (Fig 6C). These findings suggest that an increase in β-arrestin expression could enhance HIF-1 dependent transcription of VEGF-A in neoplastic and metastatic breast cancer.

Inhibition of VEGF secretion by anti-angiogenic compounds results from a disruption of β-arrestin1-HIF-1 signaling

The immunomodulatory drug thalidomide was previously shown to suppress angiogenesis, although the mechanism was not unknown (D'Amato et al., 1994; Figg, 2006; Holaday & Berkowitz, 2009). It was further suggested that thalidomide inhibits secretion of VEGF from tumors and bone marrow stromal cells leading to decreased endothelial cell migration and adhesion (Dredge et al., 2002; Vacca et al., 2005). When we treated MDAMB-231 cells with thalidomide, we saw a complete inhibition of hypoxia-induced HIF-1-dependent transcription as measured by 5XHRE luciferase reporter activity (Fig 7A). Paradoxically, HIF-1α stabilization during hypoxia was not affected and similar amounts of HIF-1α were detected in cell extracts with or without thalidomide treatment (Fig 7B). However, when we analyzed β-arrestin1 distribution in thalidomide-treated cells we observed a predominant cytoplasmic translocation of endogenous β-arrestin1 from the nucleus and only 10–15% protein remained in the nucleus as assessed by immunostaining (Fig 7C). Furthermore, while hypoxia induced a robust HIF-1α and β-arrestin1 colocalization in the nuclear compartment, addition of thalidomide under hypoxia resulted in relocation of β-arrestin1-HIF-1 complexes to the perinuclear compartments (Fig 7D). Additionally, the tyrosine kinase inhibitor, imatinib mesylate, which has been shown to exhibit anti-angiogenic effects (Vlahovic et al., 2006) caused a similar mislocalization of β-arrestin1-HIF-1α into perinuclear compartments (Fig 7D). However, unlike thalidomide, treatment of MDAMB-231 cells with imatinib inhibited the accumulation of HIF-1α during hypoxia (Fig 7E). These data strongly suggest that β-arrestin1-HIF-1 interaction in the nucleus is required for inducing VEGF transcription and secretion in carcinoma cells. Moreover, drugs that can cause nuclear export of β-arrestin1 could prove useful in reducing gene transcription during hypoxia and serve as inhibitors of breast cancer angiogenesis.

DISCUSSION

Recent studies have indicated that in addition to the neoplastic role played by GPCRs and G proteins in a variety of cancers (Daaka, 2004), β-arrestins may also play a crucial role in the progression of colorectal, ovarian and lung cancer in mice (Buchanan et al., 2006; Raghuwanshi et al., 2008; Rosano et al., 2009). We have found that β-arrestin1 regulates breast cancer cell survival during hypoxia through a novel interaction with the transcription factor, HIF-1. Additionally, our analyses of human breast tumors indicate that an up regulation of β-arrestin1 correlates with an increase in VEGF-A, a key regulator of tumor angiogenesis. Our data also establishes that nuclear export of β-arrestin1 disrupts HIF-1-dependent transcription of VEGF-A, and that formation and localization of β-arrestin-HIF-1α complexes could be fundamental for cell survival during hypoxia.

Thus far, few studies have addressed the mechanistic role of β-arrestins in promoting nuclear transcription (Kang et al., 2005). However, its role in inhibiting nuclear transcription has dominated among the spectrum of its recently discovered functions (DeWire et al., 2007). The finding that β-arrestin1 binds and potentiates HIF-1 activity provides an exciting and unexpected view of how signal transduction during hypoxia might be regulated. We propose that β-arrestin1 acts as a scaffolding protein for recruiting and stabilizing HIF-1 and thus regulating gene transcription during hypoxia. Whether this involves binding of β-arrestin1 with other co-factors to promote HIF-1α and HIF-1β dimerization or whether β-arrestin1 prevents binding of repressor elements that inhibit HIF-1 activity remains to be determined. Nonetheless, our findings demonstrate a novel role of β-arrestin1 in promoting expression of the HIF-1 transcriptional target VEGF-A.

VEGF-A belongs to a family of cytokines that bind to and activate VEGF receptors to stimulate proliferation, migration and recruitment of endothelial cells (Ferrara et al., 2003; Leung et al., 1989). VEGFA-VEGFR2 interaction plays a crucial role in both developmental and pathological angiogenesis and there is increased expression of these molecules in many solid tumors. The importance of targeting tumor angiogenesis was suggested in early 1970's (Folkman et al., 1971) and has since led to cancer drugs targeting this pathway, such as Bevacizumab (a humanized monoclonal antibody that binds VEGFA), VEGF-Trap (soluble fusion proteins of extra cellular domains of VEGFRs1 and 2 and the Fc portion of human IgG), Sunitinib (VEGFR and RTK inhibitor) (Holaday & Berkowitz, 2009). These molecules bind either the VEGF ligand or its receptor and thus prevent signal transduction that is required for endothelial cell proliferation and subsequent angiogenesis. Previous studies have also shown that thalidomide (that has re-emerged as a drug for multiple myeloma) and imatinib (that inhibits c-Abl and other tyrosine kinases) reduce the accumulation of VEGF as well as inhibit tumor angiogenesis and growth, although the exact mechanism was not known (Beppu et al., 2004; D'Amato et al., 1994; Ebos et al., 2002; Figg, 2006; Holaday & Berkowitz, 2009; Vlahovic et al., 2006),. Our studies reveal that these latter two compounds prevent β-arrestin1-HIF1α interaction in the nuclear compartment during hypoxia and inhibit VEGF transcription. In summary, our findings strongly suggest that β-arrestin1 has a pro-angiogenic role in breast carcinoma, and predictably, drugs that inhibit its nuclear activity or stimulate nuclear export could be useful in inhibiting breast cancer angiogenesis and metastasis.

Materials and Methods

Reagents

Cell lines—MDAMB-231 cells were obtained from American Type Tissue Culture Collection and maintained in Leibowitz's L15 medium, supplemented with 14 mM $NaHCO_3$ and 10% fetal bovine serum and grown at 37 °C, 5% CO_2. MDAMB-231 and 4T1 cells stably transfected with luciferase were generously provided by Dr. P. Casey (Kelly et al., 2006). HEK-293 cells from ATCC were cultured in MEM supplemented with 10 % fetal bovine serum. Normal breast epithelial cells (Hs 578Bst, ATCC) were grown in ATCC Hybri-Care Medium supplemented with 1.5 g/L sodium bicarbonate, 30 ng/ml mouse EGF and 10% fetal bovine serum.

Plasmids—Flag-β-arrestin1, Flag-β-arrestin2 and 5XHRE-luciferase plasmids have been previously described (Moeller et al., 2004; Shenoy et al., 2008). Q394L mutation in Flag-β-arrestin1 was introduced by site-directed mutagenesis.

Antibodies—Anti-β-arrestin1 and anti-β-arrestin2 antibodies have been previously described (Attramadal et al., 1992) and were a generous gift from Dr. R. J. Lefkowitz. Other anti-β-arrestin antibodies include monoclonal anti-β-arrestin1 (BD Biosciences) and K-16 goat polyclonal antibody (SantaCruz). Rabbit polyclonal anti-HIF-1α (Novus biological) were used for immunoblotting and mouse monoclonal anti-HIF-1α (SantaCruz) was used for immunostaining and immunoprecipitation. Anti-VEGF-A antibody (mouse monoclonal C-1, SantaCruz) was used in immunostaining procedures.

siRNA—Double-stranded siRNAs were chemicallysynthesized, in deprotected and desalted form (DHARMACON). Sequences of siRNA oligonucleotides are

1. Control (CTL): AAUUCUCCGAACGUGUCACGU
2. β-arrestin2 (human): GGACCGCAAAGUGUUUGUG
3. β-arrestin1 (human): AAAGCCUUCUGCGCGGAGAAU
4. β-arrestin1 and 2 (human): ACCTGCGCCTTCCGCTATG
5. β-arrestin1 (mouse): AAAAGGAACUCUGUGCGGCUA

Immunoprecipitation and Immunoblotting

Binding between endogenous or overexpressed β-arrestin and endogenous HIF-1α was analyzed by immunoprecipitation after chemical cross-linking using Dithio-bis-maleimidoethane (DTME, Pierce). Monolayers of MDAMB-231 cells on 150 mm dishes were incubated in 21% O_2 (normoxia), 1% O2 (hypoxia) or treated with 100 μM CoCl2 (hypoxia-mimetic) for 5 hours. Next the cells were washed with phosphate buffered saline (pH 7.5) containing 10 mM HEPES (pH 7.5) (PBS/HEPES) and incubated in PBS/HEPES along with 2mM DTME (dissolved in 50% DMSO) on a rotator platform at room temperature. After 30 min, excess crosslinker was removed by washing the cells twice with PBS/HEPES and cells scraped into 1 mL RIPA buffer containing protease inhibitors. After rotating the cell extracts at 4 oC for 1–2 hours, clarified cell extracts were subjected to

immunoprecipitation. To isolate nuclear proteins for IP, first cells were subjected to lysis with a hypotonic buffer (10 mM HEPES-KOH pH 7.9, 1.5 mM $MgCl_2$, 10 mM KCl, 0.5 mM DTT, 0.2 mM PMSF). Lysed cells were incubated on ice for 10 min and NP40 was added (final 0.3%) after which nuclei were precipitated by centrifugation. The nuclei were washed once with PBS, nuclear proteins were solubilized in RIPA buffer and used for immunoprecipitation. To immunoprecipitate β-arrestin, 2 μg anti-β-arrestin antibody (K-16, SantaCruz) and protein A/G conjugated agarose were mixed with 800 μg of cellular protein. To isolate HIF-1α IPs, 3 μg of anti-HIF-1α antibody, ProteinA/G conjugated agarose and 800 μg of cellular protein were used. To test the role of NES in HIF-1 binding, MDAMB-231 cells were transfected with β-arrestin1-Flag, β-arrestin1 (Q394L)-Flag or β-arrestin2-Flag (5 μg/150 mm dish) with Lipofectamine2000 reagent. 48h after transfection, cells were exposed to hypoxia as above and harvested in RIPA buffer. Soluble cell extracts weremixed with anti-Flag M2 agarose beads and rotated overnight at 4 °C. Nonspecific binding in the IPs was eliminated by repeated wash and centrifugation steps. Samples were eluted with SDS-sample buffer and separated on SDS-PAGE and transferred to nitrocellulose membrane for Western blotting. For protein detection in the IPs containing endogenous proteins, Protein-A-HRP was used instead of a HRP conjugated secondary IgG (Lal et al., 2005). Chemiluminescence detection was performed using SuperSignal®West Pico or Femto reagent (Pierce). Signals were quantified by densitometry using Quantity One software (BioRad)..

Immunostaining

Cells were plated on collagen-coated35-mm glass bottom plates and incubated in 21% O_2 (normoxia), 1% O2 (hypoxia) or treated with 100 μM CoCl2 (hypoxia-mimetic) for 5 hours. Following this, cells were fixed with 5% formaldehyde dilutedin PBS containing calcium and magnesium, permeabilizedwith 0.08% Triton X-100™ (cat# T-9284, Sigma) in PBS containing 2% bovine serum albuminfor 30 min and incubated with appropriateprimary antibody O/N at 4°C, followed by the respective secondary antibody. To label β-arrestin1, anti-β-arrestin1 antibody (A1CT) was used at 1:300 dilution in 2 % BSA followed by Alexa Fluor® 488 goat anti-rabbit IgG (H+L). HIF-1α was detected with a mouse monoclonal anti-HIF-1α antibody (1:300 dilution) followed by Alexa Fluor® 594 goat anti-mouse IgG (H+L). Confocal images were obtained on a Zeiss LSM510 laser-scanning microscope usingmultitrack sequential excitation (488 and 568 nm) andemission (515–540 nm, GFP; 585–615 nm, Texas Red) filter sets using either 100X or 40 X oil immersion objectives.

Breast tissue sections on Zymed MaxArray Human Breast Carcinoma (60 cancer cores plus 1 normal tissue) and IMGENEX HISTO-Array tissue microarray slides (50 cancer cores plus 10 normal) were deparaffinized and rehydrated. After this the sections were incubated in a blocking buffer (3% BSA) in a humidified chamber. β-arrestin1 and HIF-1α were immunostained as above. To detect β-arrestin2, anti-β-arrestin2 antibody A2CT (1:250 dilution) was used. VEGF-A was detected with a mouse monoclonal antibody followed by Alexa Fluor® 594 goat anti-mouse IgG (H+L) and nuclei were labelled with DRAQ5 (Alexis Corporation). Confocal images were acquired in a random order for different samples in a tissue microarray by high-resolution confocal microscopy (Zeiss LSM 510, and 40X or 100X oil immersion objective). Sections that were stained only with secondary

antibodies served as negative controls. Pixel intensities for different fluorophore signals in each image were determined with the MetaMorph software.

Luciferase Reporter Assay

MDAMB-231 cells were transfected with luciferase reporter plasmid alone or with different siRNA oligonucleotides (control, βarr1, βarr2 or βarr1/2) using Lipofectamine 2000. 48 hours later transfected cells were plated on 24-well dishes. Next day cells were serum-starved for 1–2 h and incubated at 1% O_2 or treated with 100 μM $CoCl_2$ for 5h. After this, cells were lysed, collected and assayed using a Luciferase Reporter Assay Kit (Promega) according to the included protocol.

Viability Assays

MDAMB-231 cells were transfected with control, βarr1 or βarr2 siRNA and 48h after transfection were split into 24-well dishes. Cells were incubated at 1% O2 or treated with 100 μM CoCl2, after which the ATP content was measured with CellTiter-Glo® luminescent cell viability assay kit (Promega) according to the included protocol.

In Vivo measurements

Adult female nude mice used in the animal studies were purchased from Charles River. All animal experiments complied with Duke University Institutional Animal Care and Use Committee guidelines. 1×10^6 MDAMB-231-luciferase cells or 50,000 4T1-luciferase cells were used per tail vein injection. A highly sensitive cooled CCD camera mounted in a light-tight box (IVIS; Xenogen), was used to perform bioluminescent imaging on animals that were anesthetized with 1–3% isoflurane. The acquisition and analysis software Living Image® (Xenogen) controlled Imaging and quantification of signals. Prior to imaging each animal was injected with D-luciferin at 100 mg/kg i.p. Light emitted from the bioluminescent tumors cells was detected by the IVIS camera system, integrated, digitized, and displayed. Regions of interest (ROI) from displayed images were marked surrounding regions with luminescence and quantified as total photons/s using Living Image® software (Xenogen). Since the imaging was noninvasive, the same animals were analyzed for tumor growth up to 30–35 days after which animals had to be euthanized for humane reasons.

Supplementary Material

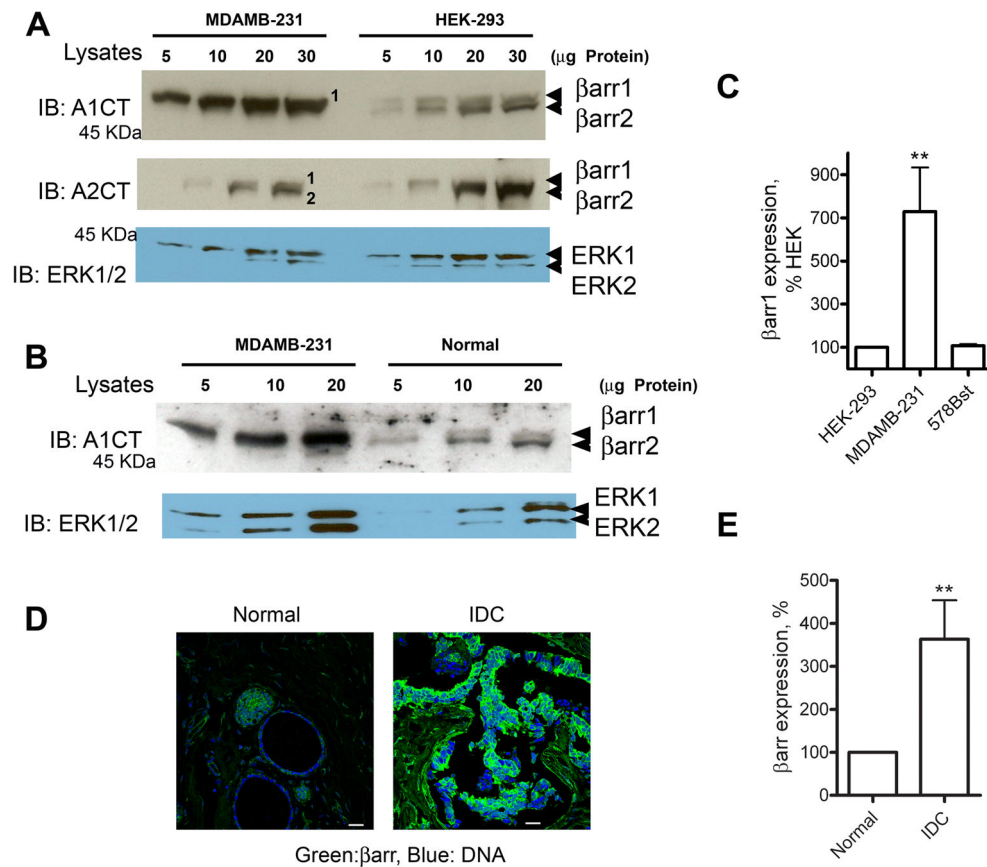Refer to Web version on PubMed Central for supplementary material.
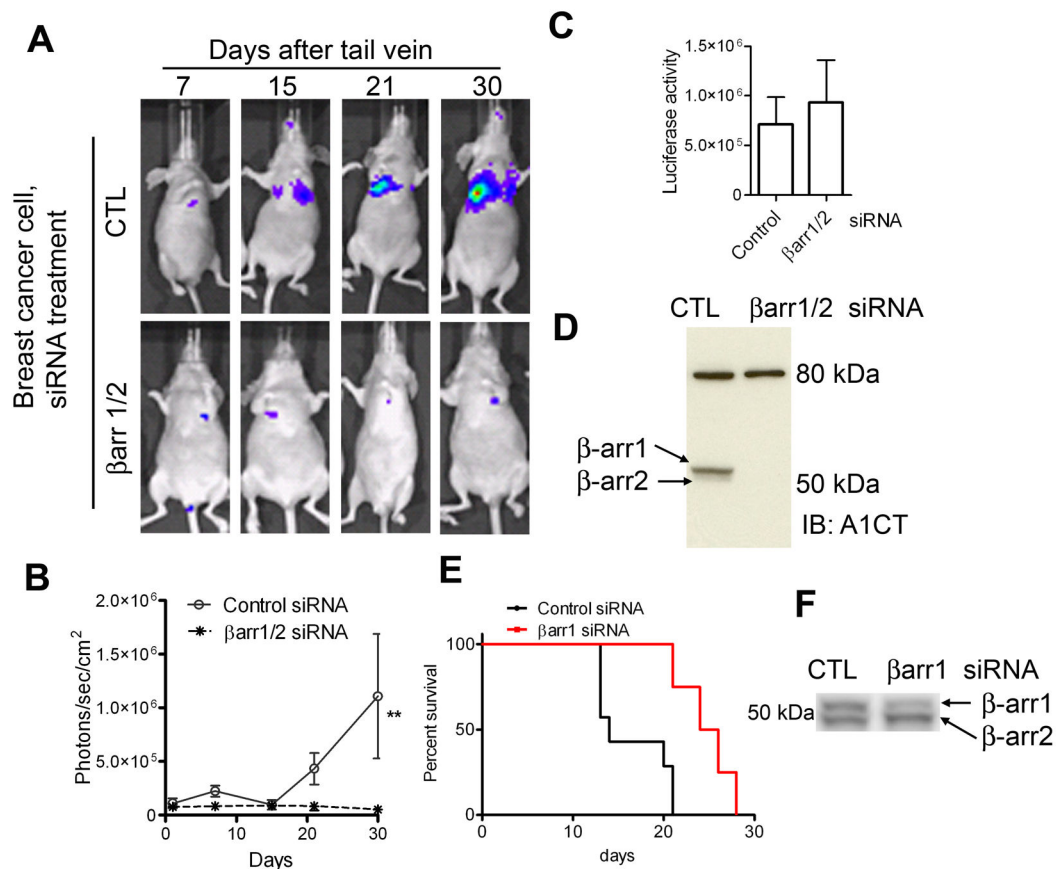
Acknowledgments

References

Alvarez CJ, Lodeiro M, Theodoropoulou M, Camina JP, Casanueva FF, Pazos Y. Endocr Relat Cancer. 2009; 16:599–611. [PubMed: 19153210]

Arany Z, Huang LE, Eckner R, Bhattacharya S, Jiang C, Goldberg MA, Bunn HF, Livingston DM. Proc Natl Acad Sci U S A. 1996; 93:12969–73. [PubMed: 8917528]

Attramadal H, Arriza JL, Aoki C, Dawson TM, Codina J, Kwatra MM, Snyder SH, Caron MG, Lefkowitz RJ. J Biol Chem. 1992; 267:17882–90. [PubMed: 1517224]

Beppu K, Jaboine J, Merchant MS, Mackall CL, Thiele CJ. J Natl Cancer Inst. 2004; 96:46–55. [PubMed: 14709738]

Buchanan FG, Gorden DL, Matta P, Shi Q, Matrisian LM, DuBois RN. Proc Natl Acad Sci U S A. 2006; 103:1492–7. [PubMed: 16432186]

Chuaqui RF, Zhuang Z, Emmert-Buck MR, Liotta LA, Merino MJ. Am J Pathol. 1997; 150:297–303. [PubMed: 9006344]

D'Amato RJ, Loughnan MS, Flynn E, Folkman J. Proc Natl Acad Sci U SA. 1994; 91:4082–5.

Daaka Y. Sci STKE. 2004:re2. [PubMed: 14734786]

Dasgupta P, Rastogi S, Pillai S, Ordonez-Ercan D, Morris M, Haura E, Chellappan S. J Clin Invest. 2006; 116:2208–2217. [PubMed: 16862215]

DeWire SM, Ahn S, Lefkowitz RJ, Shenoy SK. Annu Rev Physiol. 2007; 69:483–510. [PubMed: 17305471]

Dredge K, Marriott JB, Macdonald CD, Man HW, Chen R, Muller GW, Stirling D, Dalgleish AG. Br J Cancer. 2002; 87:1166–72. [PubMed: 12402158]

Ebos JM, Tran J, Master Z, Dumont D, Melo JV, Buchdunger E, Kerbel RS. Mol Cancer Res. 2002; 1:89–95. [PubMed: 12496355]

Ferrara N, Gerber HP, LeCouter J. Nat Med. 2003; 9:669–76. [PubMed: 12778165]

Figg WD. Clin Pharmacol Ther. 2006; 79:1–8. [PubMed: 16413236]

Folkman J, Merler E, Abernathy C, Williams G. J Exp Med. 1971; 133:275–88. [PubMed: 4332371]

Gavard J, Gutkind JS. Nat Cell Biol. 2006; 8:1223–34. [PubMed: 17060906]

Ge L, Shenoy SK, Lefkowitz RJ, DeFea K. J Biol Chem. 2004; 279:55419–24. [PubMed: 15489220]

Girnita L, Shenoy SK, Sehat B, Vasilcanu R, Vasilcanu D, Girnita A, Lefkowitz RJ, Larsson O. J Biol Chem. 2007; 282:11329–38. [PubMed: 17303558]

Holaday JW, Berkowitz BA. Mol Interv. 2009; 9:157–66. [PubMed: 19720747]

Kang J, Shi Y, Xiang B, Qu B, Su W, Zhu M, Zhang M, Bao G, Wang F, Zhang X, Yang R, Fan F, Chen X, Pei G, Ma L. Cell. 2005; 123:833–47. [PubMed: 16325578]

Kelly P, Moeller BJ, Juneja J, Booden MA, Der CJ, Daaka Y, Dewhirst MW, Fields TA, Casey PJ. Proc Natl Acad Sci U S A. 2006; 103:8173–8. [PubMed: 16705036]

Kohout TA, Lin FS, Perry SJ, Conner DA, Lefkowitz RJ. Proc Natl Acad Sci U S A. 2001; 98:1601–6. [PubMed: 11171997]

Kvietikova I, Wenger RH, Marti HH, Gassmann M. Nucleic Acids Res. 1995; 23:4542–50. [PubMed: 8524640]

Lakshmikanthan V, Zou L, Kim JI, Michal A, Nie Z, Messias NC, Benovic JL, Daaka Y. Proc Natl Acad Sci U S A. 2009; 106:9379–84. [PubMed: 19458261]

Lal A, Haynes SR, Gorospe M. Mol Cell Probes. 2005; 19:385–8. [PubMed: 16146684]

Lefkowitz RJ, Rajagopal K, Whalen EJ. Mol Cell. 2006; 24:643–52. [PubMed: 17157248]

Lefkowitz RJ, Shenoy SK. Science. 2005; 308:512–7. [PubMed: 15845844]

Letessier A, Sircoulomb F, Ginestier C, Cervera N, Monville F, Gelsi-Boyer V, Esterni B, Geneix J, Finetti P, Zemmour C, Viens P, Charafe-Jauffret E, Jacquemier J, Birnbaum D, Chaffanet M. BMC Cancer. 2006; 6:245. [PubMed: 17040570]

Leung DW, Cachianes G, Kuang WJ, Goeddel DV, Ferrara N. Science. 1989; 246:1306–9. [PubMed: 2479986]

Li TT, Alemayehu M, Aziziyeh AI, Pape C, Pampillo M, Postovit LM, Mills GB, Babwah AV, Bhattacharya M. Mol Cancer Res. 2009; 7:1064–77. [PubMed: 19609003]

Liu Y, Cox SR, Morita T, Kourembanas S. Circ Res. 1995; 77:638–43. [PubMed: 7641334]

Ma XJ, Salunga R, Tuggle JT, Gaudet J, Enright E, McQuary P, Payette T, Pistone M, Stecker K, Zhang BM, Zhou YX, Varnholt H, Smith B, Gadd M, Chatfield E, Kessler J, Baer TM, Erlander MG, Sgroi DC. Proc Natl Acad Sci U S A. 2003; 100:5974–9. [PubMed: 12714683]

Maxwell PH, Wiesener MS, Chang GW, Clifford SC, Vaux EC, Cockman ME, Wykoff CC, Pugh CW, Maher ER, Ratcliffe PJ. Nature. 1999; 399:271–5. [PubMed: 10353251]

Minn AJ, Gupta GP, Siegel PM, Bos PD, Shu W, Giri DD, Viale A, Olshen AB, Gerald WL, Massague J. Nature. 2005; 436:518–24. [PubMed: 16049480]

Moeller BJ, Cao Y, Li CY, Dewhirst MW. Cancer Cell. 2004; 5:429–41. [PubMed: 15144951]

Mythreye K, Blobe GC. Proc Natl Acad Sci U S A. 2009; 106:8221–6. [PubMed: 19416857]

Niida A, Smith AD, Imoto S, Aburatani H, Zhang MQ, Akiyama T. BMC Bioinformatics. 2009; 10:71. [PubMed: 19243633]

Raghuwanshi SK, Nasser MW, Chen X, Strieter RM, Richardson RM. J Immunol. 2008; 180:5699– 706. [PubMed: 18390755]

Rosano L, Cianfrocca R, Masi S, Spinella F, Di Castro V, Biroccio A, Salvati E, Nicotra MR, Natali PG, Bagnato A. Proc Natl Acad Sci U S A. 2009; 106:2806–11. [PubMed: 19202075]

Scott MG, Le Rouzic E, Perianin A, Pierotti V, Enslen H, Benichou S, Marullo S, Benmerah A. J Biol Chem. 2002; 277:37693–701. [PubMed: 12167659]

Semenza GL. Sci STKE. 2007:cm8. [PubMed: 17925579]

Shenoy SK, Xiao K, Venkataramanan V, Snyder PM, Freedman NJ, Weissman AM. J Biol Chem. 2008; 283:22166–76. [PubMed: 18544533]

Vacca A, Scavelli C, Montefusco V, Di Pietro G, Neri A, Mattioli M, Bicciato S, Nico B, Ribatti D, Dammacco F, Corradini P. J Clin Oncol. 2005; 23:5334–46. [PubMed: 15939924]

Vlahovic G, Rabbani ZN, Herndon JE 2nd, Dewhirst MW, Vujaskovic Z. Br J Cancer. 2006; 95:1013– 9. [PubMed: 17003785]

Wang GL, Jiang BH, Rue EA, Semenza GL. Proc Natl Acad Sci U S A. 1995; 92:5510–4. [PubMed: 7539918]

Wang GL, Semenza GL. J Biol Chem. 1995; 270:1230–7. [PubMed: 7836384]

Wang P, Wu Y, Ge X, Ma L, Pei G. J Biol Chem. 2003; 278:11648–53. [PubMed: 12538596]

Zou L, Yang R, Chai J, Pei G. Faseb J. 2008; 22:355–64. [PubMed: 17890288]

Figure 1.
A) Indicated amounts of cell extracts of MDAMB-231 and HEK-293 cells were analyzed by Western blotting using the rabbit polyclonal antibodies anti-β-arrestin1 (A1CT, top panel) and anti-β-arrestin2 (A2CT, middle panel) generated against carboxyl terminal domains of β-arrestin1 and β-arrestin2, respectively. The two antibodies have five-fold more affinity toward the cognate antigen isoform than the other (Kohout et al., 2001). The bottom panel shows relative amounts of ERK 1 and 2 (as a loading control) in the lysate samples. **B)** Indicated amounts of cell extracts of MDAMB-231 and normal breast epithelial cells (Hs 578Bst, ATCC) were immunoblotted for β-arrestins with A1CT antibody (top panel) and ERK (lower panel). **C)** Protein bands were quantified from three to four independent experiments, normalized to protein (μg) input and plotted as bar graphs. ** $p < 0.01$, carcinoma cells versus others, one-way ANOVA, Bonferroni post test. **D)** Immunostaining of human breast tissue sections (Zymed breast tissue arrays) for βarr1 expression. Representative confocal micrographs shown were obtained using LSM 510 microscope; identical instrumental settings were used to acquire images for both samples (scale bar = 20 μm). **E)** The pixel intensities for βarr immunostaining from tissue sections of normal and invasive ductal carcinoma (IDC) samples were quantified using MetaMorph, normalized to DNA content detected by DRAQ5 labeling and plotted as bar-graphs. ** $p = 0.0084$, t test, two-tailed, n = 10.

Figure 2.
A) Breast carcinoma cells with stable luciferase expression (231-luc) were transfected with control (targeting no mRNA) or βarr1/2 targeting siRNA and then injected into nude mice 50h later. The spread of luciferase-tagged cells was determined by *in vivo* bioluminescence imaging after D-luciferin i.p. injection. The time course of luminescence representing tumor growth is shown in panel 'A'. One representative mouse each from 'control cells' group and 'βarrestin-depleted cells' group are shown for the indicated time points. **B)** Quantification of luminescence from 14 mice injected with cells transfected with control siRNA-cells versus 14 mice that received cells depleted of β-arrestins using the Living Image acquisition and analysis software (Xenogen). ** $p < 0.01$ by Two-way ANOVA. **C)** Luciferase activity of respective aliquots of control and βarr1/2-depleted cells that were used for injections, as assayed with a luminometer. **D)** Western blot analyses of lysates of respective samples of injected cells. The top bands are nonspecific bands, which also serve as loading controls. **E)** For survival rate, mice ($n = 7$ for control and $n = 8$ for β-arrestin1-depleted) were injected with 4T1 cells via tail vein as described above and observed up to 35 days. Mice injected with cells depleted of β-arrestin1 displayed increased survival ($P = 0.0006$, Log-rank test) compared with mice injected with cells expressing normal amounts of β-arrestin1. **F)** An aliquot of 4T1 cells transfected with either control or β-arrestin1 siRNA was immunoblotted with A2CT antibody.
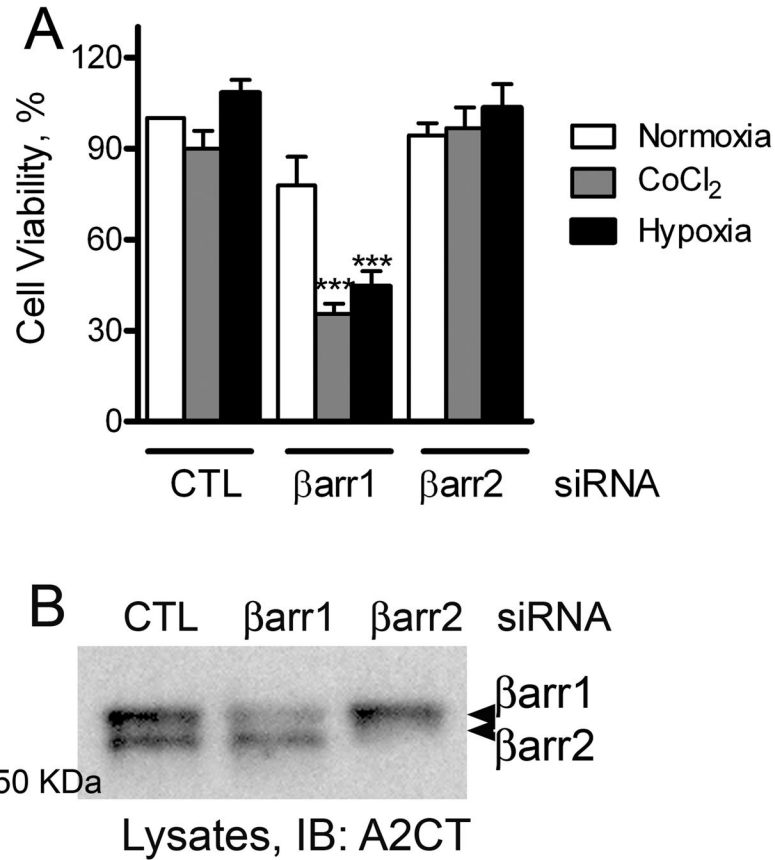
Figure 3.
A) MDAMB-231 cells transfected with siRNA targeting either no mRNA (= control, CTL), βarr1 or βarr2 were treated with 100 μM CoCl2 or grown under 1% O2. Untreated cells grown under normal oxygen levels represent the normoxia condition. 24 hours later, the amount of ATP was determined using CellTiter-Glo reagent (Promega). Cell viability was calculated as percentage ATP present according to the manufacturer's protocol. The data presented are mean ± SEM from three experiments. *** $p < 0.001$ versus control or β-arr2 group, one-way ANOVA, Bonferroni post test. **B)** Western blots show the efficiency of siRNA-mediated knockdown of individual βarrestin isoforms.
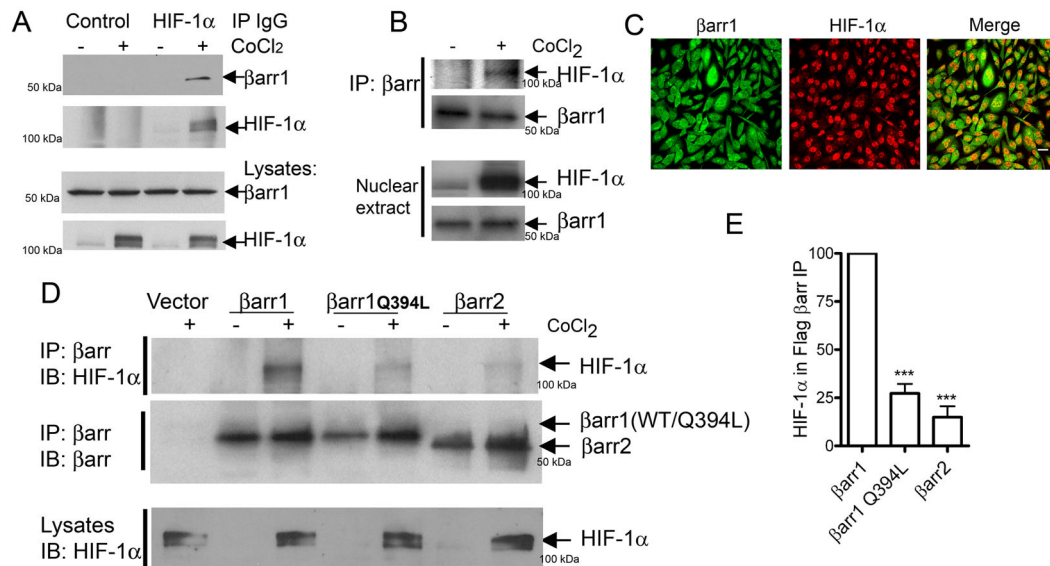
Figure 4.
A) MDAMB-231 cells were treated with vehicle or CoCl$_2$ for 6h and cell lysates were immunoprecipitated with normal mouse IgG (control) or with anti-HIF-1α mouse monoclonal IgG (28b, SantaCruz Biotech) and the immunoprecipitates (IPs) were probed for bound β-arrestin1. The blots are representative of three independent experiments. **B)** Nuclear β-arrestin1 from untreated or CoCl$_2$-treated cells (MDAMB-231) was immunoprecipitated with an anti-βarr antibody (K-16, SantaCruz Biotech) and the IPs were probed with anti-HIF-1α antibody. Representative blots are shown from one of two similar experiments. **C)** Confocal images depict immunostaining for β-arrestin1 (green) and HIF-1α (red) in MDAMB-231 cells treated with CoCl$_2$. (scale bar = 20 μm). **D)** MDAMB-231 cells were transfected with indicated plasmids encoding Flag-tagged β-arrestins. The top panel shows the amount of HIF-1α bound to Flag-βarr IPs. The middle panel shows the amount of βarr in each IP sample. Lowest panel displays detection of HIF-1α in CoCl$_2$-treated lysate samples. **E)** HIF-1α in βarr IP was quantified and normalized to βarr levels. *** $p < 0.001$, versus βarr1, Bonferroni post test, one-way ANOVA, n=4.
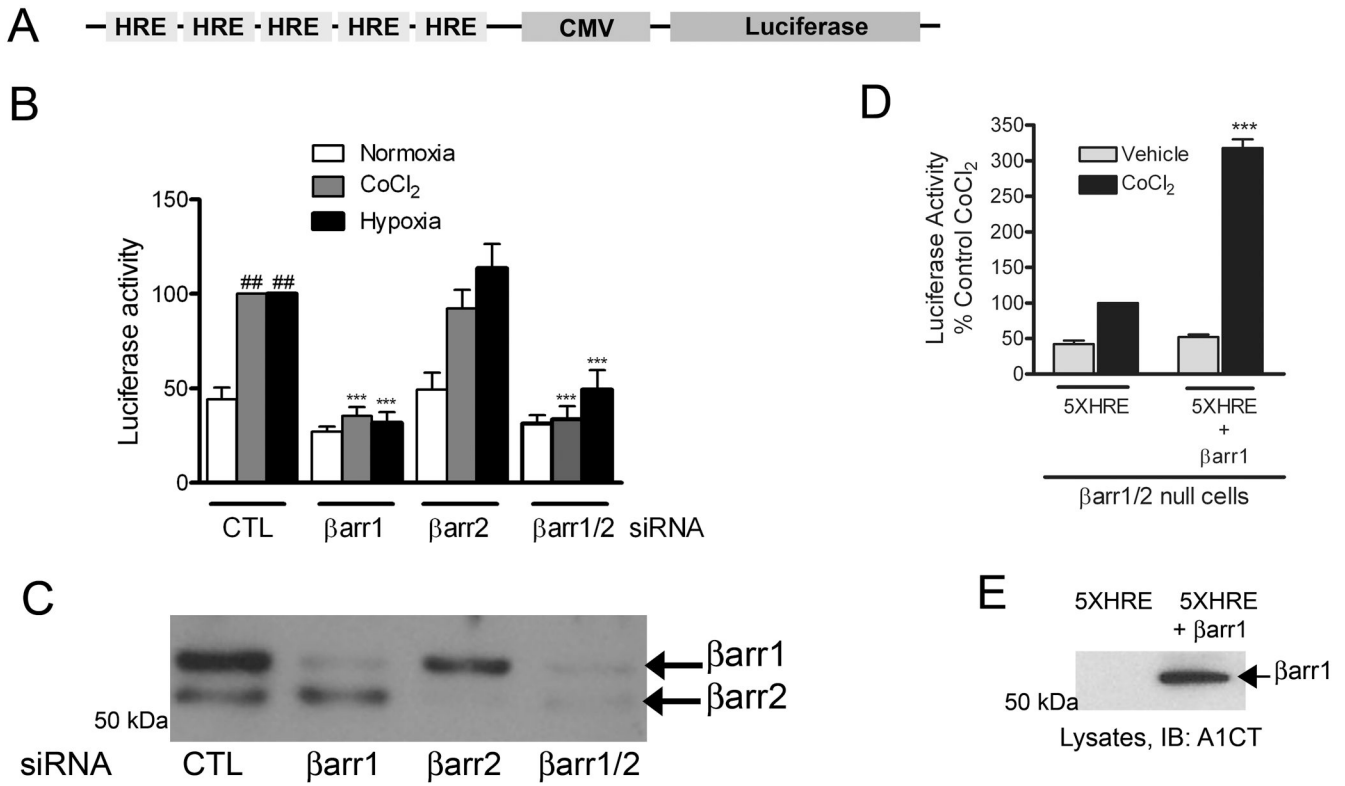
Figure 5.
A) Schematic map of luciferase reporter used; HRE: hypoxia responsive element, CMV: cytomegalovirus immediate-early gene promoter. **B)** Assay of hypoxia-induced luciferase activity upon indicated siRNA transfection. ## $p < 0.001$, versus CTL-normoxia; *** $p < 0.001$ versus CTL-CoCl$_2$ or CTL-low O$_2$, one-way ANOVA, Bonferroni post test. **C)** Western blot showing the efficiency of knockdown of each βarr isoform. **D)** Assay of hypoxia induced luciferase reporter activity in Mouse Embryonic Fibroblasts (MEFs) that are null for both βarr1 and 2 under control and βarr1 replete conditions. *** $p < 0.001$, between the two cobalt-treated samples, Bonferroni post test, one-way ANOVA, n=3. **E)** Western blot of lysates showing expression of transfected βarr1.
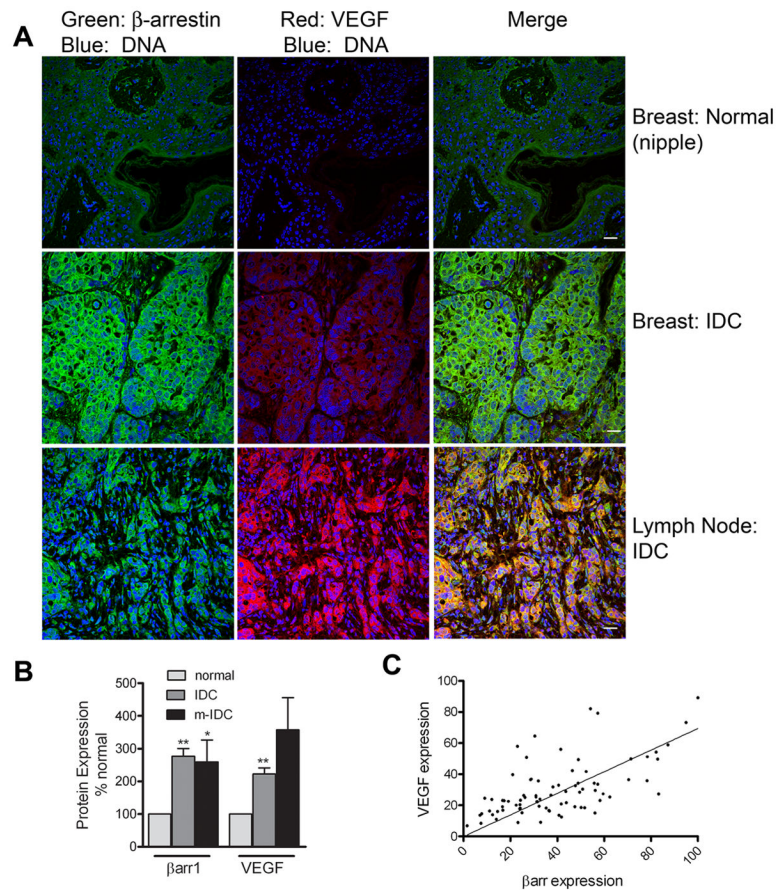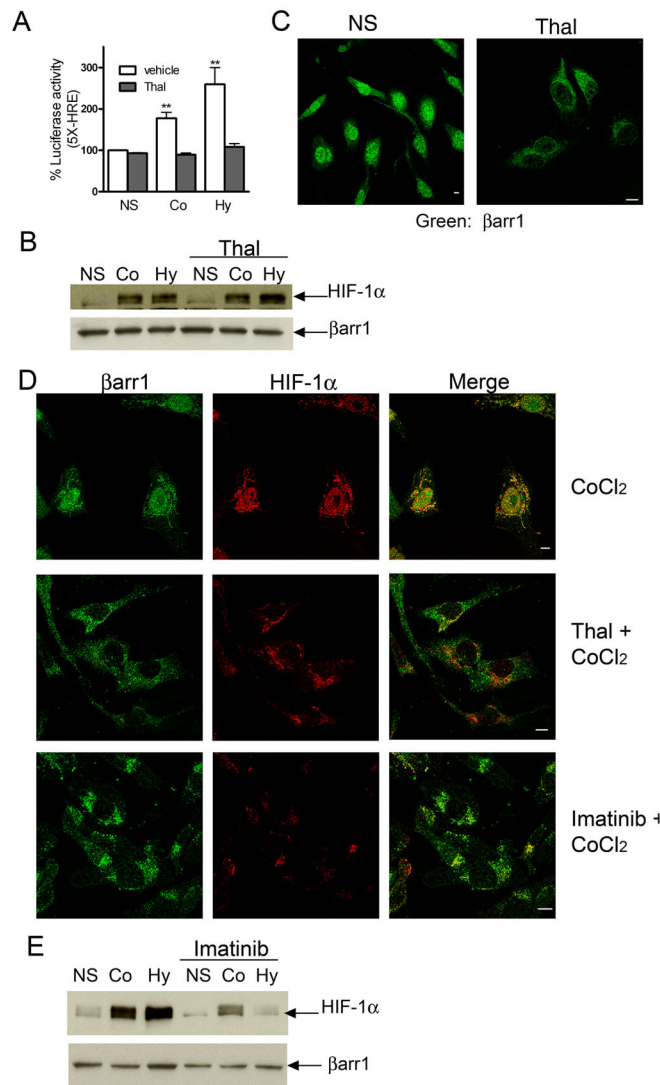
Figure 6.
A) Confocal micrographs showing β-arrestin1 (green), VEGF-A (red) and DNA labeled with DRAQ5™ (blue) from normal breast tissue (top panels), infiltrating ductal carcinoma, IDC, (middle panels) and metastatic-IDC, from lymph nodes (lowest panels). Scale bar = 20 μm. **B)** Signals from each channel were quantified using MetaMorph and plotted as bar graphs. Both β-arrestin1 and VEGF-A levels were increased more than 3- fold and significantly higher (* $p < 0.05$, ** $p < 0.01$ in IDC: n=79 tissue samples, 112 images than in normal breast tissues: n=10 tissue samples, 22 images). **C)** A correlation plot showing expression levels of β-arrestin and VEGF-A in IDCs. The values plotted are normalized signal intensities quantified by MetaMorph in 79 immunostained sections tested above.

Figure 7.
A) MDAMB-231 cells were transfected with 5X-HRE-luciferase and the extent of transcriptional activity was determined after indicated treatment as in Fig 5. ** $p < 0.01$ versus NS, one-way ANOVA, Bonferroni post test. **B)** Cells were treated as indicated and whole cell extracts were analyzed for HIF-1α and βarr1 by Western blotting. **C)** Untreated or thalidomide (20 μM) treated MDAMB-231 cells were immunostained for β-arrestin levels and confocal images were obtained as in Fig 4B. **D)** MDAMB-231 cells were treated for 5 hours with $CoCl_2$ alone or $CoCl_2$ plus thalidomide (20 μM) or imatinib (20 μM), immunostained for βarrestin (A1CT) and HIF-1α and analyzed by confocal microscopy. **E)** MDAMB-231 cells extracts were analyzed by Western blotting for HIF-1α (top) and βarr1 (bottom) after indicated treatments. Scale bars in the confocal panels = 10 μm.